Finite-Difference Time-Domain Simulation of Arbitrary Impedance using One Port S-Parameter

Joshua M. Kast and Atef Z. Elsherbeni

Department of Electrical Engineering
Colorado School of Mines, Golden, CO 80401, USA
jkast@mines.edu, aelsherb@mines.edu

Abstract ─ Many modern radio-frequency devices comprise both lumped-element components and complex geometries. Simulation of such a device requires modeling the electromagnetic interactions with both geometric features and lumped components. We present a method for including arbitrary lumped-element components into finite-difference time-domain (FDTD) simulations. The lumped-element components, which are described by their scattering parameters, are modeled in the Yee grid as dependent voltage sources. The mathematical formulation is described, along with its implementation into a FDTD simulator. For verification, simulation results of resistive, capacitive, and inductive loads are presented, and are compared to simulation results from previous lumped-element FDTD methods. This represents a first-step in modeling multiport networks described by their scattering parameters.

Index Terms ─ Circuit analysis, computational electromagnetics, fast Fourier transform, finite-difference time-domain (FDTD), linear lumped circuit, scattering parameters, stripline circuit.

I. INTRODUCTION

The finite-difference time-domain (FDTD) technique is used to simulate the behavior of electric and magnetic fields in regions comprising arbitrary materials and geometries. In addition to modelling basic materials and geometries, the FDTD technique has been extended to model voltage and current sources, lumped-elements [1], active devices [2], and arbitrary impedances [3]. Such extensions to the fundamental FDTD method increase its utility in modelling real-world electronic devices. In this work, we present a new approach to the simulation of arbitrary impedances based on their S-parameter representation.

Several descriptions exist for the representation of S-parameter defined loads in the FDTD grid [4]–[8], which utilize a transformation from S-parameters to admittance (Y) parameters. The method we describe here is most similar to the voltage-source based approaches described by Kuo et al. [9], which describes a network through its impedance (Z) parameters, and uses a dependant voltage source to simulate the arbitrary impedance. We extend the technique of [9] by providing a model which easily integrates into an existing FDTD code [1], and naturally extends to the simulation of networks spanning multiple cells. An impedance-based formulation was selected because it allows for the use of a current probe and dependent voltage source, two commonplace FDTD simulation elements, without the need to write a specialized electric field updating equation.

Commonly available commercial and open-source FDTD packages implement varying capabilities for simulation of arbitrary impedances. While formulations for arbitrary one- and two-port impedances are described in the literature, these are not commonly implemented in FDTD packages. The commercial packages Remcom's XFDTD [10] and Keysight's EMPro [11] allow the embedding of RLC impedances into a domain, but not arbitrary S-Parameters. Similarly, CEMS software [12] allows the incorporation of RLC impedances as well as diodes into FDTD domains. The open-source MEEP [13] and OpenEMS [14] packages do not have support for embedding either S-parameter nor RLC impedances into FDTD domains.

The formulation we describe in this paper is applicable to situations where an FDTD simulation domain contains a one-port passive circuit element which is defined by its S-parameter representation. In this case, the S-parameters may be applied directly to the simulation, without a need to approximate the circuit component with a combination of lumped-elements or geometric features.

II. FORMULATION

In the FDTD time-marching loop, electric fields are updated by means of the Maxwell's equation for magnetic field:

$$\nabla \times \vec{H} = \epsilon \frac{\partial \vec{E}}{\partial t} + \sigma^e \vec{E} + \vec{J}_i. \tag{1}$$

Submitted On: February 25, 2020
Accepted On: July 19, 2020

https://doi.org/10.47037/2020.ACES.J.350902

Calculated magnetic fields are in-turn used to update electric fields:

$$\nabla\times\vec{E}=-\mu\frac{\partial\vec{H}}{\partial t}-\sigma^{m}\vec{H}-\vec{M}_{i}. \tag{2}$$

Here, $\vec{E}$ and $\vec{H}$ represent the electric and magnetic fields, respectively, as vector quantities. We denote the electrical conductivity of the medium as σ^{e}, and the induced current as $\vec{J}_{i}$. The value for magnetic current, M_{i} need not be considered in the simulations below.

By expanding the curl ($\nabla\times$) operator, we may separate (1) and (2) into 6 separate equations. Taking equation (1) and considering the calculation for only the Z component of the electric field, we get the equation:

$$\frac{\partial E_{z}}{\partial t}=\frac{1}{\epsilon_{z}}\left(\frac{\partial H_{y}}{\partial x}-\frac{\partial H_{x}}{\partial y}-\sigma_{z}^{e}E_{z}-J_{iz}\right). \tag{3}$$

The FDTD method requires that equations be discretised for computation in a 3D rectangular grid. Following the formulation of [1], we re-formulate (3) with spatial coordinates discretised to cell indices *i*, *j*, and *k*, and time discretised into time-steps denoted as *n*. With this modification, the derivatives are translated into central differences. For a Z-directed electric field at time-step $n+1/2$, we get:

$$\begin{aligned}E_{z}\big|_{i,j,k}^{n+1}=&\frac{2\epsilon_{z}\big|_{i,j,k}-\Delta t\,\sigma_{z}^{e}\big|_{i,j,k}}{2\epsilon_{z}\big|_{i,j,k}+\Delta t\,\sigma_{z}^{e}\big|_{i,j,k}}E_{z}\big|_{i,j,k}^{n}\\&+\frac{2\Delta t\left(H_{y}\big|_{i,j,k}^{n+\frac{1}{2}}-H_{y}\big|_{i-1,j,k}^{n+\frac{1}{2}}\right)}{\Delta x\left(2\epsilon_{z}\big|_{i,j,k}+\Delta t\,\sigma_{z}^{e}\big|_{i,j,k}\right)}\\&-\frac{2\Delta t\left(H_{x}\big|_{i,j,k}^{n+\frac{1}{2}}-H_{x}\big|_{i,j-1,k}^{n+\frac{1}{2}}\right)}{\Delta y\left(2\epsilon_{z}\big|_{i,j,k}+\Delta t\,\sigma_{z}^{e}\big|_{i,j,k}\right)}\\&-\frac{2\Delta t}{2\epsilon_{z}\big|_{i,j,k}+\Delta t\,\sigma_{z}^{e}\big|_{i,j,k}}J_{iz}\big|_{i,j,k}^{n+\frac{1}{2}}.\end{aligned} \tag{4}$$

Equation (4) generally describes the updating of the electric field within the FDTD grid. However, a specific behavior is required for a region defined by an S-parameter. Specifically, we create a region which exerts a voltage in response to the current passing through it in the Z direction. The measurement of this current, calculation of the voltage, and application to the FDTD cell are presented below.

For a region designated as a voltage source with voltage V_{s} at time $n+1/2$, we may write the conducted current J_{iz} as:

$$J_{iz}\big|_{i,j,k}^{n+\frac{1}{2}}=\frac{I_{z}\big|_{i,j,k}^{n+\frac{1}{2}}}{\Delta x\Delta y}=\frac{\Delta V+V_{s}\big|_{i,j,k}^{n+\frac{1}{2}}}{R_{s}}, \tag{5}$$

where ΔV is the potential difference which may already exist across the cell, which is calculated by:

$$\Delta V=\Delta z\frac{E_{z}\big|_{i,j,k}^{n+1}+E_{z}\big|_{i,j,k}^{n}}{2}. \tag{6}$$

In (6), we use the time average of two electric field values, because the electric field at time-step *n* is not precisely known. Combining (6) with (5) and (4), we get a general equation for a cell containing a voltage source:

$$\begin{aligned}E_{z}\big|_{i,j,k}^{n+1}=&\\&\frac{2\epsilon_{z}\big|_{i,j,k}-\Delta t\,\sigma_{z}^{e}\big|_{i,j,k}-\dfrac{\Delta t\Delta z}{R_{s}\Delta x\Delta y}}{2\epsilon_{z}\big|_{i,j,k}+\Delta t\,\sigma_{z}^{e}\big|_{i,j,k}+\dfrac{\Delta t\Delta z}{R_{s}\Delta x\Delta y}}E_{z}\big|_{i,j,k}^{n}\\&-\frac{2\Delta t\,V_{s}\big|_{i,j,k}^{n+\frac{1}{2}}}{R_{s}\Delta x\Delta y\left(2\epsilon_{z}\big|_{i,j,k}+\Delta t\,\sigma_{z}^{e}\big|_{i,j,k}+\dfrac{\Delta t\Delta z}{R_{s}\Delta x\Delta y}\right)}\\&+\frac{2\Delta t\left(H_{y}\big|_{i,j,k}^{n+\frac{1}{2}}-H_{y}\big|_{i-1,j,k}^{n+\frac{1}{2}}\right)}{\Delta x\left(2\epsilon_{z}\big|_{i,j,k}+\Delta t\,\sigma_{z}^{e}\big|_{i,j,k}+\dfrac{\Delta t\Delta z}{R_{s}\Delta x\Delta y}\right)}\\&-\frac{2\Delta t\left(H_{x}\big|_{i,j,k}^{n+\frac{1}{2}}-H_{x}\big|_{i,j-1,k}^{n+\frac{1}{2}}\right)}{\Delta y\left(2\epsilon_{z}\big|_{i,j,k}+\Delta t\,\sigma_{z}^{e}\big|_{i,j,k}+\dfrac{\Delta t\Delta z}{R_{s}\Delta x\Delta y}\right)}.\end{aligned} \tag{7}$$

In the case of this work, a voltage source with internal resistance is generally not needed. By taking the limit of (7) as R_{s} approaches zero, we get the formulation for a hard voltage source:

$$E_{z}\big|_{i,j,k}^{n+1}=-E_{z}\big|_{i,j,k}^{n}-\frac{2}{\Delta z}V_{s}\big|_{i,j,k}^{n+\frac{1}{2}}. \tag{8}$$

We attempt to simulate a linear lumped network by means of this voltage source. Therefore, we must calculate the value of V_{s} at each time-step, in response to the current through the network. The frequency response of a one-port RF network may be defined by its reflection coefficient Γ, which is obtained from the S-parameter S_{11}. For a network excited by a sinusoidal voltage at frequency f ($\tilde{V}(f)$), the relationship between voltage and current at a given frequency is described as [15]:

$$Z(f)=\frac{\tilde{V}(f)}{\tilde{I}(f)}=Z_{0}\frac{1+S_{11}(f)}{1-S_{11}(f)}. \tag{9}$$

For clarity, we may rewrite (9) as:

$$\tilde{V}(f)=\tilde{I}(f)Z_{11}(f). \tag{10}$$

Equation (10) describes the relationship of frequency-domain quantities of voltage and current. However, for FDTD simulation, we require voltage to be calculated in the time-domain. Taking the inverse Fourier transform of (10), we find that the operation of multiplication has transformed into convolution of

current and impedance:

$$V(t) = I(t) * \mathbb{F}^{-1}\{Z_{11}(f)\}. \quad (11)$$

While other methods [4-6], [8-9] make use of polynomial approximations of the circuit impedance, the use of convolution allows truly arbitrary impedances to be simulated, at a moderate cost in computation time. We will define the symbol $\hat{z}_{11}(t)$ as the inverse Fourier transform of $Z_{11}(f)$, giving:

$$V(t) = I(t) * \hat{z}_{11}(t). \quad (12)$$

To calculate voltage, it is necessary to measure the current through the cell at each time-step. This is accomplished by the integral form of Ampere's law:

$$I_{\text{free}} = \oint \vec{H} \cdot dl. \quad (13)$$

Applied to the Yee grid, (13) becomes:

$$\begin{aligned} I_z\big|_{is:ie,\,js:je,k}^{n+\frac{1}{2}} &= \Delta x \sum_{i=is}^{ie} \left(H_x\big|_{i,\,js-1,k}^{n+\frac{1}{2}} - H_x\big|_{i,\,je,k}^{n+\frac{1}{2}} \right) \\ &+ \Delta y \sum_{j=js}^{je} \left(H_y\big|_{ie,\,j,k}^{n+\frac{1}{2}} - H_y\big|_{is-1,\,j,k}^{n+\frac{1}{2}} \right). \end{aligned} \quad (14)$$

For accurate calculation of the current through the cell, the values of *is*, *js*, *ie*, and *je* are chosen to bound the cell containing the hard voltage source, with an additional margin of 1 cell in each direction. At each time-step, (14) is evaluated and the result saved in an array with current values for previous time-steps, enabling the convolution in (12) to be computed:

$$\begin{aligned} &V_s\big|_{i,\,j,k}^{n+\frac{1}{2}} = \\ &\sum_{m=1}^{n} I_s\big|_{is:ie,\,js:je,k}^{m+\frac{1}{2}} \hat{z}_{11}\left(\left(n-m+\frac{1}{2} \right) \Delta t \right). \end{aligned} \quad (15)$$

The complete updating equation for the S-parameter defined cell may now be written as:

$$\begin{aligned} &E_z\big|_{i,\,j,k}^{n+1} \\ &= -E_z\big|_{i,\,j,k}^{n} \\ &-\frac{2}{\Delta z} \sum_{m=1}^{n} I_s\big|_{is:ie,\,js:je,k}^{m+\frac{1}{2}} \hat{z}_{11}\left(\left(n-m+\frac{1}{2} \right) \Delta t \right). \end{aligned} \quad (16)$$

It is important to note that the notation $I_s\big|_{is:ie,\,js:je,k}^{m+\frac{1}{2}}$ in (16) refers to the array containing all computed values of current from the beginning of the simulation to the current time-step.

III. SIMULATION CONFIGURATION

To test this formulation, an FDTD simulation was created using the MATLAB codes presented in [1], with modifications to support a voltage-source controlled by the formulation described in Section II. The configuration of the computational domain is illustrated in Fig. 1.

The circuit comprises a 20 mm length of conductive stripline suspended in a dielectric material with a permittivity of $\epsilon_r = 3.2$. Above and below the dielectric material are thin sheets modelled as perfect electric conductors. The stripline width of 1.2 mm, and the separation between the top and bottom PEC plates of 2.0 mm, was optimized in previous FDTD simulations to give an 50Ω characteristic impedance for the transmission line.

For simulation, a uniform cell size of $\Delta x = \Delta y = \Delta z = 0.1\text{mm}$ was chosen. The simulation was performed with a time step of $\Delta t = 173.325$ fs, and the domain was excited with a Gaussian pulse chosen to give a minimum of 40 cells per wavelength. For all simulations, 20000 time-steps were carried out. The domain is excited by a single voltage source in the plane of the stripline conductor, producing a Gaussian pulse of with a 1V amplitude.

IV. SIMULATION RESULTS

For the resistive circuit described below, a simulation was carried out using the lumped-element (LE-FDTD) formulation described in [1], [16], [17]. For capacitive (RC) and inductive (RL) circuits, the appropriate formulation described in [3] was simulated using the CEMS software [12].

Then the LE-FDTD, RL, or RC representation of the circuit component was replaced with a voltage source, which was updated at each time-step according to the formulation in Section II. For each simulation, voltage and current were recorded at points indicated in Fig. 1. These values are plotted in the time and frequency domain for comparison.

A. Resistive 50Ω load

To test the formulation described in Section II a simulation was carried out using an ideal 50Ω load terminating the stripline shown in Fig. 1. For a structure with $Z_0 = 50\Omega$, terminated in a 50Ω load, the S_{11} is expected to be 0 for all frequencies. Using (9), we find $Z_{11} = 50\Omega$ across all frequencies. The simulated S- parameter defined load was compared to a LE-FDTD simulated 50Ω resistor in place of the 1 port S_{11} element.

Time domain results from the simulation are plotted in Fig. 2 as voltage and current through the probes illustrated in Fig. 1. At the beginning of the simulation, the Gaussian pulse excitation pulse may be seen followed by several reflections. There is a good agreement both in magnitude and timing between the S-parameter defined load (port) of Section II and of the LE-FDTD simulation.

The time-domain results were converted to frequency-domain S-parameters for comparison, as plotted in Fig. 3. As with the time-domain results, we see good agreement between the S-parameters, both in magnitude and in phase.

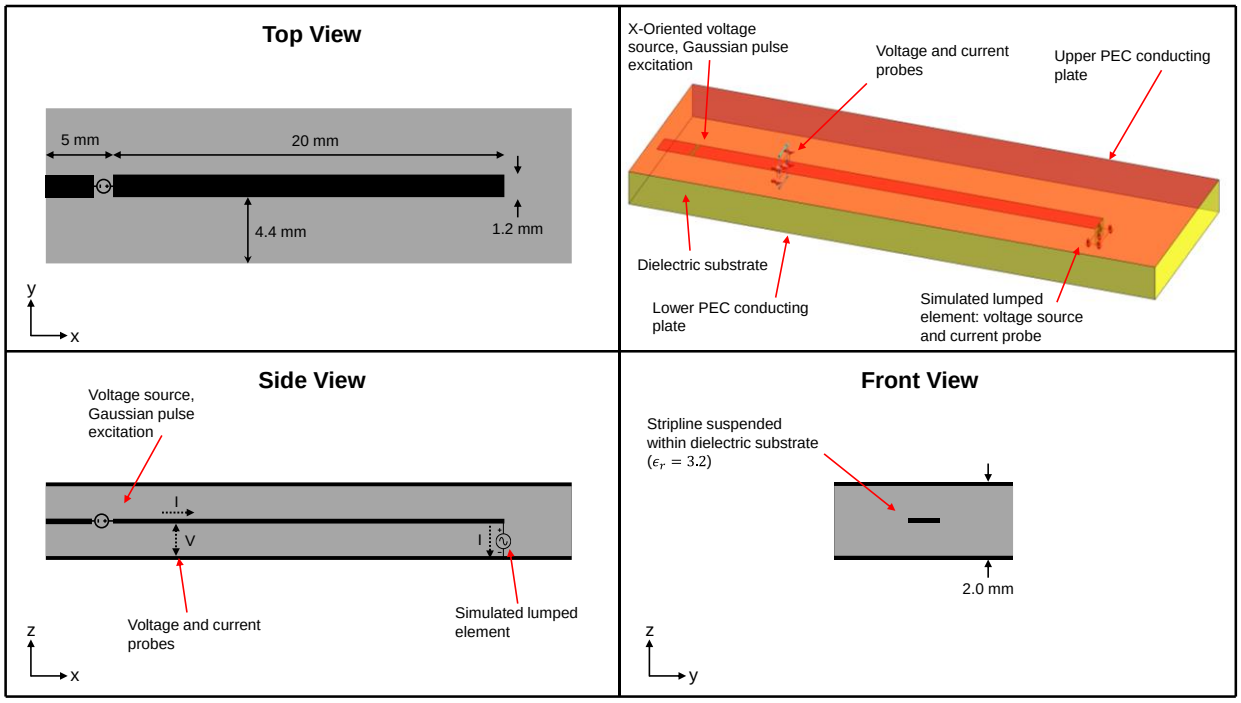

Fig. 1. Stripline configuration for FDTD simulation.

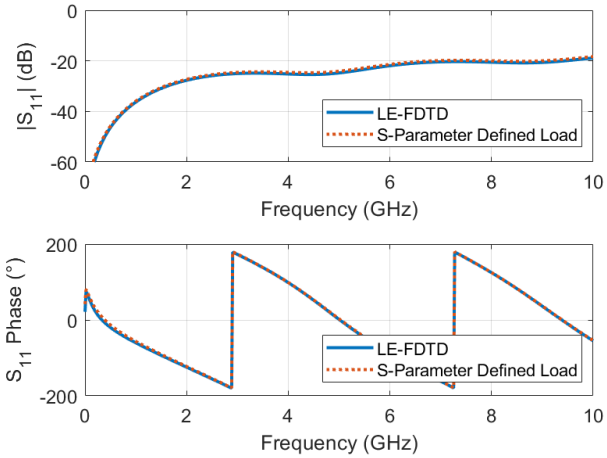

Fig. 2. Computed time-domain voltage and current based on results for lumped-element and S-parameter simulation with 50Ω resistive load.

B. Capacitive (RC) load

To further test the simulation, a lumped-load comprising a 10 µF capacitor in parallel with a 50 Ω resistor was simulated using both the S-parameter defined load and the LE-FDTD method. The S-parameters for this configuration were calculated as described in [18].

Time-domain results from this simulation are plotted in Fig. 4. As with the resistive 50Ω load case, good agreement is seen between the S-parameter defined load (port) and the LE-FDTD representations of the RC circuit. Similarly, the frequency-domain results plotted in Fig. 5 align well: at low frequencies, the impedance of the capacitor is large, and the effect of the 50Ω load dominates. At higher frequencies, the impedance of the capacitor decreases, and the reflection of the RC load decreases.

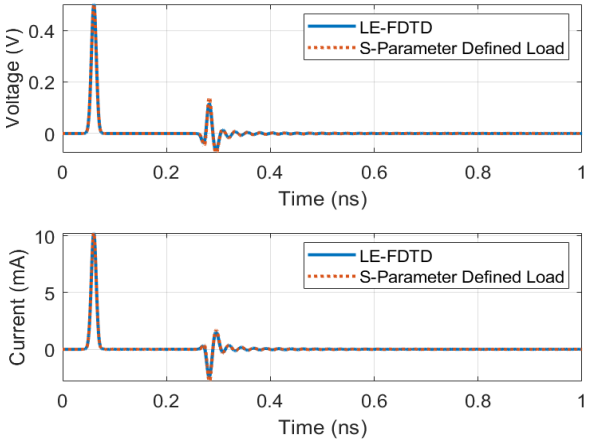

Fig. 3. Frequency-domain results from the resistive load simulation.

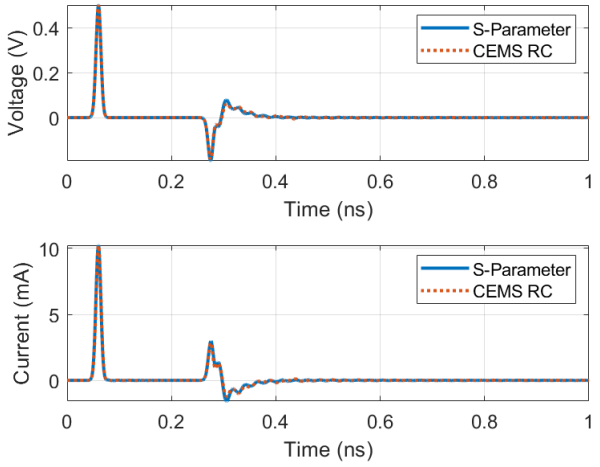

Fig. 4. Time-domain results from the RC load simulation.

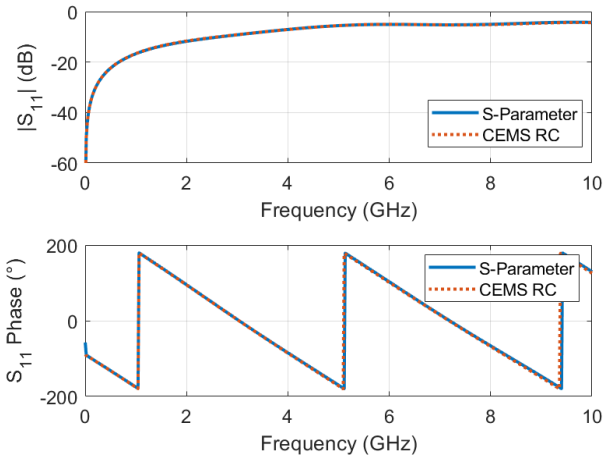

Fig. 5. Frequency-domain results from the RC load simulation.

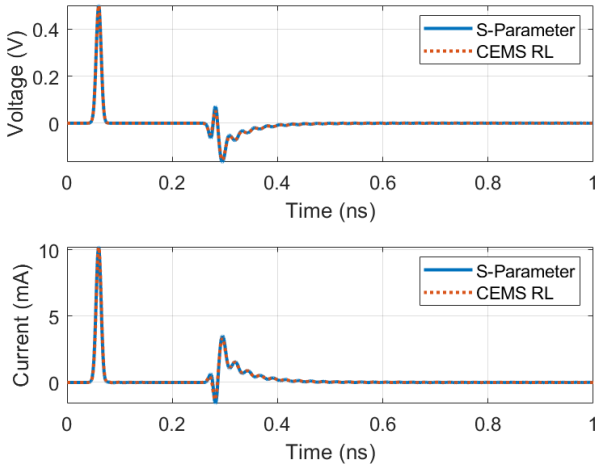

Fig. 6. Time-domain results from the RL load simulation.

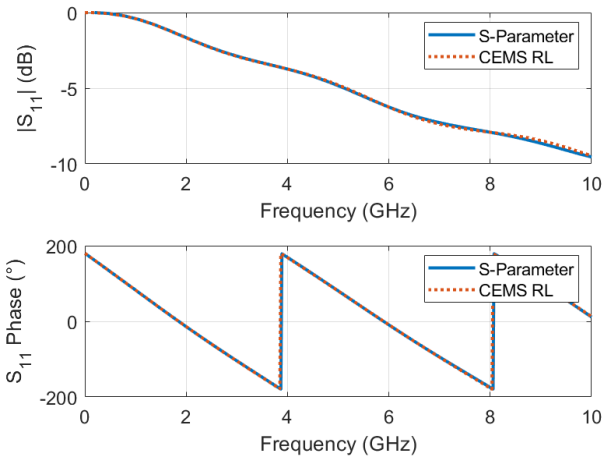

Fig. 7. Frequency domain results from the RL load simulation.

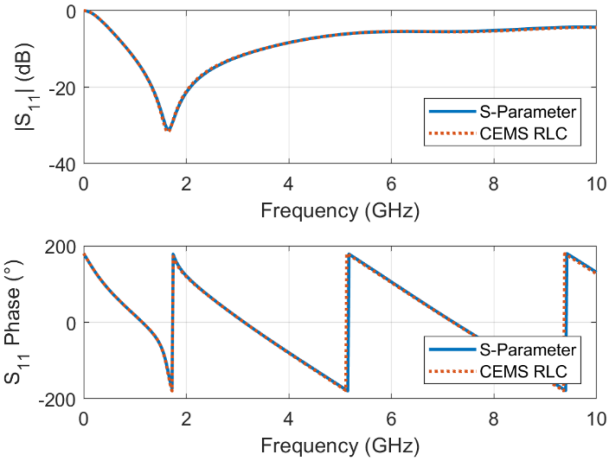

Fig. 8. Frequency-domain results from parallel RLC circuit.

C. Inductive (RL) load

An RL load comprising 50Ω resistor in parallel with a 10 nH inductor was simulated. As in the previous simulations, an LE-FDTD model was compared with an S-parameter defined load. The results from this simulation are plotted in Fig. 6 and transformed to frequency domain in Fig. 7. From the frequency-domain results, we observe the effect of the RL circuit: as frequency is increased, it becomes increasingly well-matched as the impedance of the inductor decreases.

D. Resonant (Parallel RLC) load

As a final test of the formulation, the stripline was terminated with a network comprising a 50Ω resistor, 10 nH inductor, and a 1 pF capacitor connected in parallel. Frequency-domain results from this simulation are plotted in Fig. 8. Again good agreement is obtained from the LE-FDTD model and the S-parameter simulation based on

the formulation described in this paper.

V. DISCUSSION

The formulation developed in this paper for a one port S-parameter model is used to represent resistive, capacitive, inductive, and RLC loads as terminations for a stripline transmission line FDTD simulation. These simulation results were compared to LE-FDTD simulations of the same geometries, where existing formulations for resistive capacitive, and inductive networks were used [1,3]. In all cases, good agreement is observed from the two different model simulations.

It is important to note that the agreement between the simulation results did not diminish when the complexity of the network was increased. The parallel RLC network contains two reactive components: an inductor and capacitor. This suggests that this technique may be applicable even for passive loads comprising many components in different configurations.

VI. CONCLUSION

In this work, we present an application of voltage sources and current probes, widely implemented in FDTD packages, to model arbitrary loads defined by S-parameters. By converting S-parameters to time-domain Z (impedance) parameters, it is possible to simulate the arbitrary impedance as a dependant voltage source within the FDTD grid. The method described in this paper therefore allows for embedding of an arbitrary one-port impedance into an FDTD domain, where the impedance is described in the form of its S-parameters.

REFERENCES

[1] A. Z. Elsherbeni and V. Demir, "The finite-difference time-domain method for electromagnetics with Matlab simulations," *Raleigh: The Institution of Engineering and Technology*, 2016.

[2] K. Elmahgoub and A. Z. Elsherbeni, "FDTD implementations of integrated dependent sources in full-wave electromagnetic simulations," *Applied Computational Electromagnetics Society (ACES) Journal*, vol. 29, no. 12, pp. 1093-1101, Dec. 2014.

[3] V. Demir, "Formulations for modeling voltage sources with RLC impedances in the FDTD method," *Applied Computational Electromagnetics Society (ACES) Journal*, vol. 31, no. 9, pp. 1020-1027, Sep. 2016.

[4] Y. Wang and S. Langdon, "FDTD simulation of real lumped components and RF devices," in *2016 10th European Conference on Antennas and Propagation (EuCAP)*, pp. 1-4, 2016.

[5] T.-L. Wu, S.-T. Chen, and Y.-S. Huang, "A novel approach for the incorporation of arbitrary linear lumped network into FDTD method," *IEEE Microw. Wirel. Compon. Lett.*, vol. 14, no. 2, pp. 74-76, Feb. 2004.

[6] X. Ye and J. L. Drewniak, "Incorporating two-port networks with S-parameters into FDTD," *IEEE Microw. Wirel. Compon. Lett*., vol. 11, no. 2, pp. 77-79, Feb. 2001.

[7] J. Zhang and Y. Wang, "FDTD analysis of active circuits based on the S-parameters [microwave hybrid ICs]," in *Proceedings of 1997 Asia-Pacific Microwave Conference*, vol. 3, pp. 1049-1052 1997.

[8] H. E. A. El-Raouf, W. Yu, and R. Mittra, "Application of the Z-transform technique to modelling linear lumped loads in the FDTD," *Antennas Propag. IEE Proc. - Microw*., vol. 151, no. 1, pp. 67-70, Feb. 2004.

[9] C.-N. Kuo, R.-B. Wu, B. Houshmand, and T. Itoh, "Modeling of microwave active devices using the FDTD analysis based on the voltage-source approach," *IEEE Microw. Guid. Wave Lett*., vol. 6, no. 5, pp. 199-201, May 1996.

[10] *XFDTD*, State College, PA: Remcom, 2020.

[11] *EMPrio.* Santa Rosa, CA: Keysight, 2020.

[12] V. Demir and A. Elsherbeni, "Computational Electromagntics Simulator (CEMS)," Software Package Version 4, Aug. 2020.

[13] A. Oskooi, D. Roundy, M. Ibanescu, P. Bermel, J. D. Joannopoulos, and S. G. Johnson, "MEEP: A flexible free-software package for electromagnetic simulations by the FDTD method," *Computer Physics Communications*, vol. 181, pp. 687-702, 2010

[14] T. Liebig, A. Rennings, S. Held, and D. Erni, "openEMS – A free and open source equivalent-circuit (EC) FDTD simulation platform supporting cylindrical coordinates suitable for the analysis of traveling wave MRI applications," *International Journal of Numerical Modelling: Electronic Networks, Devices and Fields*, vol. 26, no. 6, pp. 680-696, 2013.

[15] D. A. Frickey, "Conversions between S, Z, Y, H, ABCD, and T parameters which are valid for complex source and load impedances," *IEEE Trans. Microw. Theory Tech*., vol. 42, no. 2, pp. 205-211, Feb. 1994.

[16] W. Sui, D. A. Christensen, and C. H. Durney, "Extending the two-dimensional FDTD method to hybrid electromagnetic systems with active and passive lumped elements," *IEEE Trans. Microw. Theory Tech*., vol. 40, no. 4, pp. 724-730, Apr. 1992.

[17] M. Piket-May, A. Taflove, and J. Baron, "FD-TD modeling of digital signal propagation in 3-D circuits with passive and active loads," *IEEE Trans. Microw. Theory Tech*., vol. 42, no. 8, pp. 1514-1523, Aug. 1994.

[18] D. M. Pozar, *Microwave Engineering*, 4th Edition. Hoboken, NJ: Wiley, 2011.

Joshua M. Kast is a Ph.D. candidate at Colorado School of Mines, Department of Electrical Engineering. He received his Bachelor of Science degree in Chemistry, and Master of Science degree in Electrical Engineering in 2011 and 2017 respectively, both from Colorado School of Mines. His current areas of research include computational electromagnetics with emphasis on the finite-difference time-domain method, and measurement of nonlinear microwave devices.

Atef Z. Elsherbeni received an honor B.Sc. degree in Electronics and Communications, an honor B.Sc. degree in Applied Physics, and a M.Eng. degree in Electrical Engineering, all from Cairo University, Cairo, Egypt, in 1976, 1979, and 1982, respectively, and a Ph.D. degree in Electrical Engineering from Manitoba University, Winnipeg, Manitoba, Canada, in 1987. He started his engineering career as a part time Software and System Design Engineer from March 1980 to December 1982 at the Automated Data System Center, Cairo, Egypt. From January to August 1987, he was a Post-Doctoral Fellow at Manitoba University. Elsherbeni joined the faculty at the University of Mississippi in August 1987 as an Assistant Professor of Electrical Engineering. He advanced to the rank of Associate Professor in July 1991, and to the rank of Professor in July 1997. He was the Associate Dean of the college of Engineering for Research and Graduate Programs from July 2009 to July 2013 at the University of Mississippi. He then joined the Electrical Engineering and Computer Science (EECS) Department at Colorado School of Mines in August 2013 as the Dobelman Distinguished Chair Professor. He was appointed the Interim Department Head for (EECS) from 2015 to 2016 and from 2016 to 2018 he was the Electrical Engineering Department Head. In 2009 he was selected as Finland Distinguished Professor by the Academy of Finland and TEKES. Elsherbeni is a Fellow member of IEEE and ACES. He is the Editor-in-Chief for ACES Journal, and a past Associate Editor to the Radio Science Journal. He was the Chair of the Engineering and Physics Division of the Mississippi Academy of Science, the Chair of the Educational Activity Committee for IEEE Region 3 Section, the general Chair for the 2014 APS-URSI Symposium, the president of ACES Society from 2013 to 2015, and the IEEE Antennas and Propagation Society (APS) Distinguished Lecturer for 2020-2022.